

Effect of deposition parameters on kinematics growth and optical properties of Fe₂O₃ nano films deposited by PLD.

Suad Mahmood Kadhim

E-mail: dr.suadmahmood@gmail.com

Laser and Optoelectronics Engineering Department/University of Technology-
Baghdad-Iraq

Abstract:

The optical and structural properties of Fe₂O₃ thin films deposited via pulsed laser deposition (PLD) have been studied. In PLD the energy of laser pulses was varied to investigate the properties of Fe₂O₃ thin films. In this work, different thickness of Fe₂O₃ thin film are deposited on glass substrates, namely, 63 nm, 110 nm and 189 nm. The structure of Fe₂O₃ thin films is investigated by the X-Ray diffraction, and it was formed to be polycrystalline structure. The XRD measurements show that these nano films have sharp peaks at $2\theta = 25^\circ$ indicating a preferred orientation along (012) plane and the grain size (GS) increase with energy of laser pulses. The surface morphology of the deposited material has been tested via (SEM) gives good homogeneous films. According to the results, the nanoparticles GS and the thickness are ranging from (6.8 nm to 12.4 nm) and from (63 nm to 189 nm) is observed, respectively. The optical band gap of prepared films in range about (2.28-2.8eV).

Key words: Fe₂O₃ nano thin films, structure and optical properties, PLD method.

تأثير معاملات الترسيب على حركية النمو والخواص البصرية لاغشية أكسيد الحديد الثلاثي النانوية المرسبة بواسطة الترسيب الليزر النبضي.

الخلاصة:

تم دراسة الخواص البصرية والتركيبية لاغشية أكسيد الحديد الثلاثي المرسبة بواسطة الترسيب بالليزر النبضي.

في الترسيب بالليزر النبضي كانت طاقة الليزر متنوعة لاستقصى الخواص البصرية لاغشية اوكسيد الحديد. في هذا العمل استخدمت اسماك مختلفة للاغشية (63-189) نانومتر. الخواص التركيبية لاغشية اوكسيد الحديد الثلاثي درست من خلال فحص حيود الاشعة السينية وبينت انها تملك تركيب متعدد التبلور. قياسات حيود الاشعة السينية بين ان الاغشية النانوية تمتلك قمم حادة عند زاوية مساوية 25° مشيرة لافضل اتجاه عند المستوي (012) وحجم حبيبي يزداد بزيادة طاقة الليزر. تشكيلية السطح تم اختبارها عن طريق المجهر الالكتروني الماسح واعطت الاغشية تجانس جيد. وفقا لهذه النتائج فان الحجم الحبيبي والسمك بمعدل من (6.8-12.4) نانومتر و(63-189) نانومتر على التوالي. فجوة الطاقة البصرية للاغشية المحضرة فانها تتراوح من (2.28-2.8) الكترون فولت.

الكلمات المفتاحية: اغشية اوكسيد الحديد الثلاثي النانوية الرقيقة، الخواص التركيبية والبصرية، طريقة الترسيب بالليزر النبضي.

1-Introduction

Iron oxides exist in different crystal structures, namely, ferrimagnetic magnetite (Fe_3O_4), maghemite ($\gamma\text{-Fe}_2\text{O}_3$), antiferromagnetic wustite (Fe O) and hematite ($\alpha\text{-Fe}_2\text{O}_3$) [1]. The Maghemite especially used in magnetic data storage media. It is a metastable cubic spinel structure which transforms into hematite above 400°C [2]. The iron oxides are used in several electronic devices which requiring polarized or magnetic materials [3]. In addition, the

maghemite high Faraday rotation has applications in optical devices.

Furthermore, there is a little information about the optical and magnetooptical characteristics for iron oxides, especially those of the metastable maghemite phase [4]. Thus, the optical properties of the iron oxide in terms of; refractive index, absorption coefficient, and Faraday rotation have attracted attention by many researchers in order to use it in magnetooptical devices. There are several deposition techniques

are used hitherto, namely, plasma assisted molecular-beam epitaxial (MBE) [5] pulsed laser deposition (PLD) from oxide targets and reactive sputter deposition from an Fe target with Ar-O₂ mixture gas flow besides Fe₃O₄ [6], other iron oxides, Fe₂O₃, FeO, and some non-stoichiometric oxides, have been reported to be present in the deposited films, depending on the deposition conditions [7,8]. The Fe₂O₃ is brown or reddish brown and hence can be easily distinguished from the other oxides, FeO and Fe₃O₄, which are black. There are two important optical parameters for the Fe₂O₃ which are called optical constant, namely, the refractive index (n) and the extinction coefficient (k).

2-Experimental Details

A pure powder of Fe₂O₃ within a high purity of 99.99% is used as a target in order to prepare the samples. In this work, the glass

substrates are adopted for the prepared thin film utilizing the pulsed laser deposition (PLD). Both of the chemically and ultrasonically methods are adopted in order to clean the glass substrates as follow; both of the ethanol and the distill water are used to clean the glass substrate. Then, the samples are placed in beaker contain distill water inside ultrasonic device for 2 hours at 353K, the powder Fe₂O₃ was compressed by sing compression tool at pressure 160 kg and the samples were compressed in disks at a diameter of 1cm and thickness 3 mm and the substrates and target were fixed in the chamber of PLD system. The deposition chamber pressure is kept at 10⁻⁵ Torr.

2-1- Deposition of Fe₂O₃ Films:

The Fe₂O₃ was deposited on the glass substrates by using pulsed laser deposition system with temperature 300°C, the frequency

of laser (3Hz) and the number of pulses is 150 pulses. The base energy of laser was changed by

the energy (700,800 and 900mJ). The figure (1) shows pulsed laser deposition system.



Fig.(1): Schematic diagram of the PLD system.

2-2- X- Ray Diffraction Spectra:

In order to determine both of the nature and structural characteristics of the growth film, the Philips PW 1840 X – ray

$$G.S = \frac{A\lambda}{\Delta\theta \cos\theta}$$

diffractometer of $\lambda = 1.54 \text{ \AA}$ from Cu – K α is used.

The polycrystalline material GS is calculated utilizing X–ray spectrum [9]:

$$\dots (1)$$

2-3- Scanning Electron Microscope (SEM):

Morphology studies of the films on the glass substrate were

carried out scanning electron microscope (SEM) type VEGA TE SCAN, with an accelerating voltage of 30kV and magnification of 10000X.

2-4- Optical Measurements:

The optical transmission of prepared thin film is recorded via UV-VIS, Phoenix-2000V device within the optical spectrum from

$$I_t = I_o \exp(-\alpha t) \quad \dots (2)$$

where I_t is the intensity of the transmitted photon at a thickness (t) and I_o is the intensity of the incident photon at surface of material[11]:

$$A = \log(I_o/I_t) \quad \dots (3)$$

We have

$$\alpha = 2.303 A/t \quad \dots (4)$$

The reflectance (R) has been found by using the relationship:

$$R + T + A = 1 \quad \dots (5)$$

For normal reflectance, we have [12]:

$$R = (n-1)^2 / (n+1)^2 \quad \dots (6)$$

By using the above relation, the refractive index can be determined from the relation:

$$n = (1 + (R)^{1/2}) / (1 - (R)^{1/2}) \quad \dots (7)$$

The extinction coefficient k is related to the absorption coefficient by the relation:

200 nm to 1000 nm. The other optical characteristics are calculated from the followed well known formulas based on the data that extracted from the optical transmission and absorption results.

The absorption coefficient (α) is calculated from Beer–Lambert law [10]:

$$K = \alpha\lambda/4\pi \quad \dots (8)$$

Optical energy gap determined from the relation [13]:

$$\alpha = (h\nu - E_g)^{1/2} \quad \text{for } h\nu > E_g \quad \dots (9)$$

Both of the real (ϵ_r) and imaginary part (ϵ_i) of dielectric constant are calculated from [12]:

$$\epsilon_r = n_2^2 - k_2^2 \quad \dots (10)$$

$$\epsilon_i = 2nk \quad \dots (11)$$

3- Results and Discussion:

3- 1 Structural properties:

3-1-1 X-ray diffraction results:

XRD pattern of Fe₂O₃ thin film was shown in figure (2). Laser energy affects the surface morphology, and optical properties of thin films. The peaks were appearing at 2θ range of 24.16°, 33.12°, 35.63°, 40.64°, 54.08° and 58.3° can be attributed to the 012, 104, 110, 113, 116 and 112 crystalline structures corresponding to pure Fe₂O₃ thin film. From the X-Ray diffraction peaks, it could be shown that the film structure changed from an amorphous

phase to crystalline with the increased in laser energy from (700- 900mJ). Films deposited at lower laser energy have defects and impurities of interstitial atoms whose concentration decreases with an increase in laser energy density.

The crystallinity of the deposited films enhances as noticed by the sharpness of the peak corresponding to the (012) plane and the occurrence of the peak corresponding to the (104) plane as show in figure (a and b). The average crystalline size of thin film was increased with increasing in laser energy; it was calculated using equation (1).

From the results, the samples at a thickness of 63, 110 and 189 nm is produced nanoparticles within

a GS of 6.8nm, 9.7 nm and 12.4 nm, respectively.

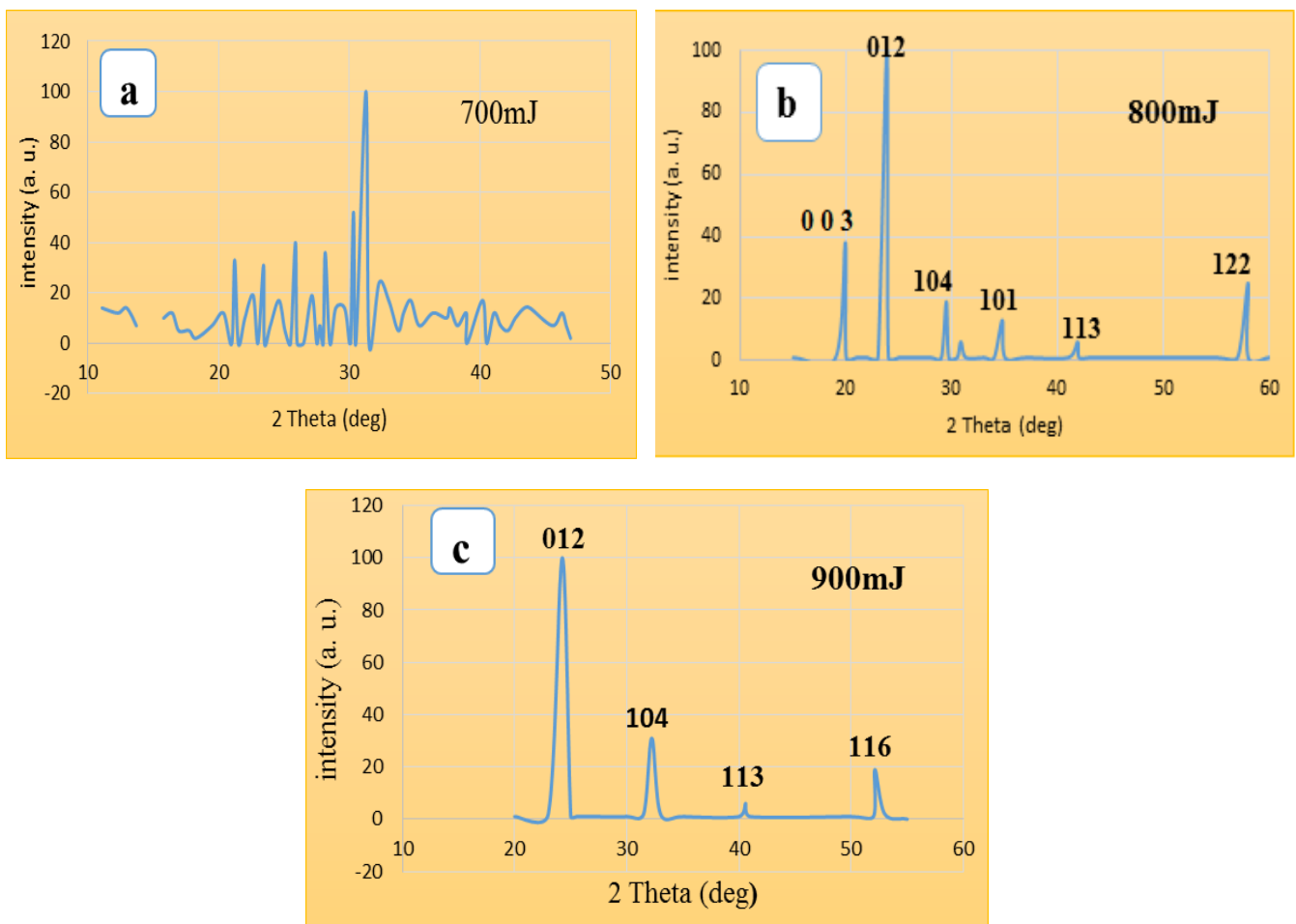


Fig.(2): X-ray diffraction pattern for Fe₂O₃ thin film.

3-1-2 Morphology results (SEM):

The surface morphological information of the prepared films is investigated via the SEM as illustrated in figure (3). According to the topographic images, the films in optimum conditions resulted in a well adherent, compact dense layer which covers the entire substrate surface, but this film has a sponge nature of elongated fibers.

The average GS which measured via SEM is larger than it

determined via XRD. This can be attributed due to the agglomeration of grains. The surface of the films is smooth and well coherence to the glass. [14]. In fig. (4) shown the grain size of the films versus of the base energy of laser pulses. Grain size was determined by using the Debye - Scherrer equation (1). Increasing of energy deposition produce an increase in the GS of the Fe_2O_3 films approximately from (6.8 to 12.4 nm) for the films deposited at (700 to 800mJ), respectively.

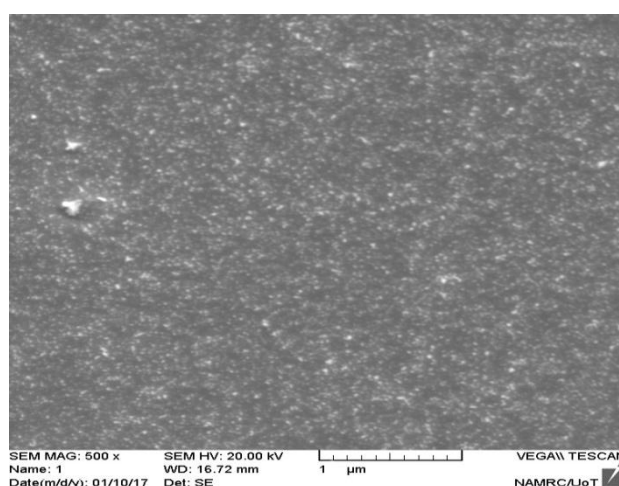


Fig.(3): Scanning electron micrograph of nano Fe_2O_3 thin film.

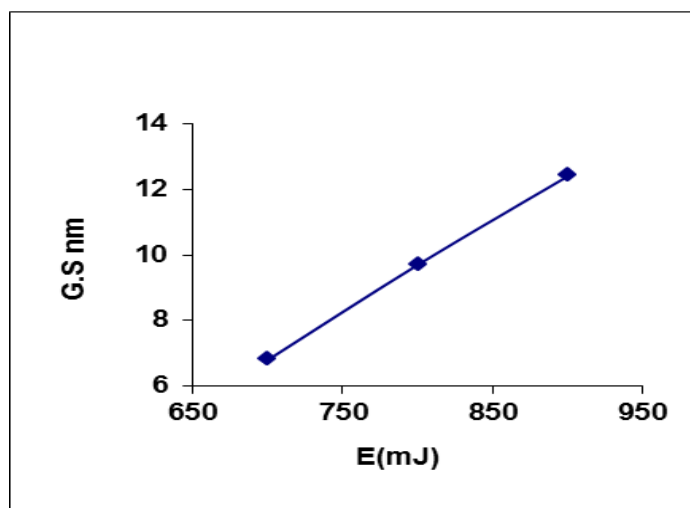


Fig.(4): The GS of nano Fe_2O_3 films versus of laser energy.

3-2 Optical Properties:

The transmittance spectrum of Fe_2O_3 films for several laser energy is depicted in figure (5). All films have high transmission at long wavelengths approximately (70 – 80 %), and decreasing transmission to (10%) at short wavelength. The

transmission of the film increases with increasing energy of laser up to (800 mJ) after which it starts decreasing with further increase in energy of laser up to (900 mJ). From the results, the optimum energy to deposit nano Fe_2O_3 film for photovoltaic applications is about 800 mJ.

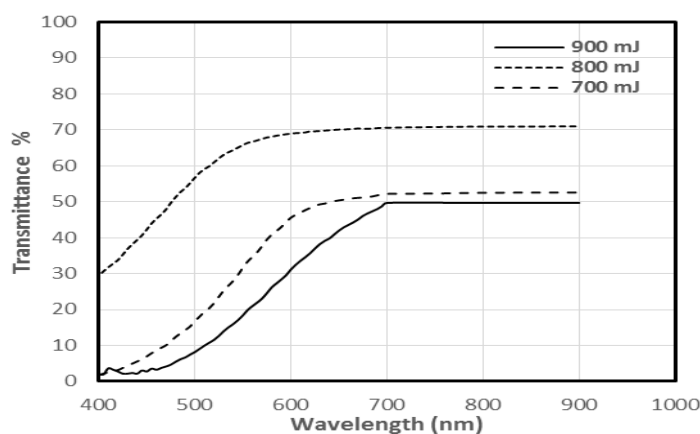


Fig. (5): The optical transmission spectrum of nano Fe_2O_3 films for different energy of laser.

Fig.(6) shows the absorbance variation versus wavelength. It is clear that the absorbance decreases when wavelength increases.

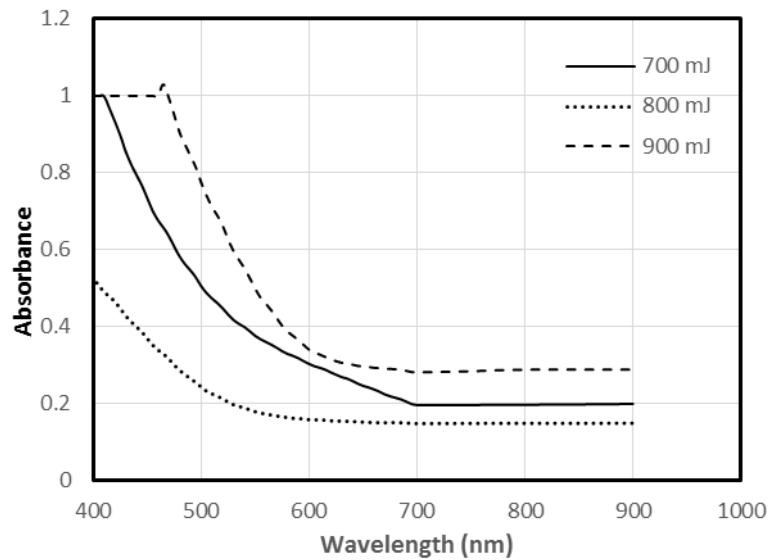


Fig.(6) :The optical absorption spectrum as a function of wavelength.

Equation (2) is used to calculate the absorption coefficient utilizing the analyzed data from the transmission spectrum. Figure (7) shows the optical absorption spectra recorded with the Fe₂O₃ films for several deposition parameters.

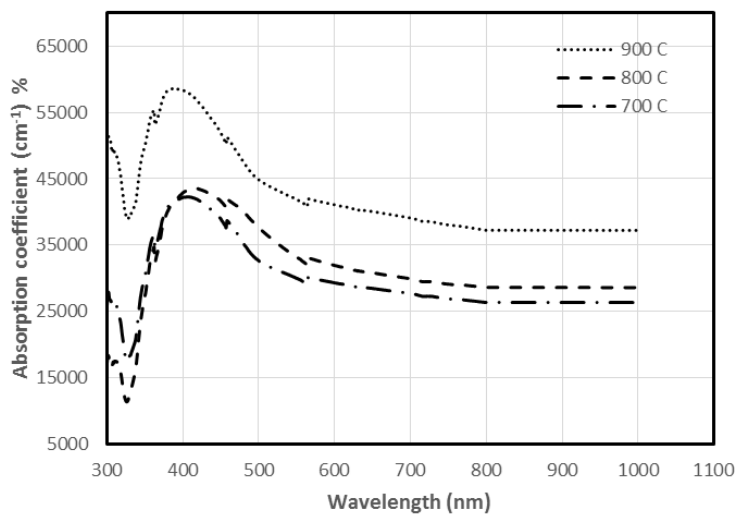


Fig.(7) The optical absorption coefficient versus wavelength of Fe₂O₃ films for different deposition parameters

The band gap depends on different parameters includes; the film structure, the arrangement and distribution of atoms in the crystal lattice. Direct and indirect energy gaps were calculated from the $(\alpha h\nu)^2$ and $(\alpha h\nu)^{1/2}$ versus photon energy respectively, according to equation (9) for several deposition parameters as illustrated in Figure (8). The band

gap value was determined via extrapolating the linear region of the curves until they intercept the photon energy axis. The linear dependence of $(\alpha h\nu)^2$ with $h\nu$ indicates $h\nu$ is the direct energy gap. It can be observed from Figure (8) that the energy gap decreases with the increasing energy of laser pulses.

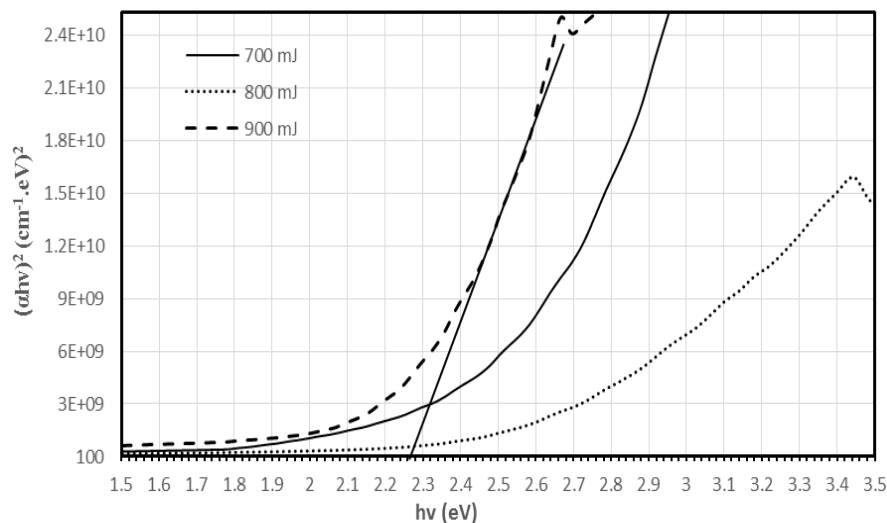


Fig. (8) A plots of $(\alpha h\nu)^2$ versus $h\nu$ of Fe_2O_3 films for several laser energy.

The extinction coefficient represents the electromagnetic wave attenuation that is propagating through the material, where it values depends on both of the density of free electrons

and structural nature of the material [15]. The extinction coefficient was evaluated using the relation (8) as a function of photon energy for several deposition parameters which is

depicted in figure (9). The values of extinction coefficient are directly related to the absorption of light. For all deposition parameters, it can be noticed that

there is a slight increase of extinction coefficient values at energies higher than (2.25 eV). After that, there is an increase with increasing photon.

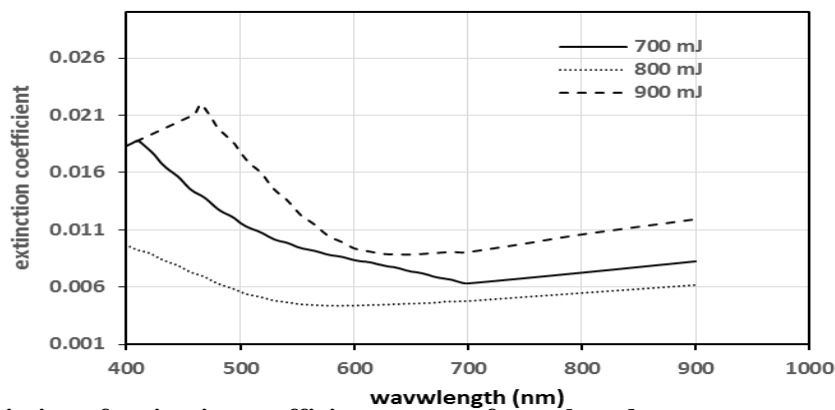


Fig.(9):Variation of extinction coefficient versus of wavelength.

The refractive index was determined from the reflectance data and equation (7). The increase of the film thickness causes an overall decrease in the

refractive index. The decrease is due to the overall decrease in the reflectance with the increase of film thickness.

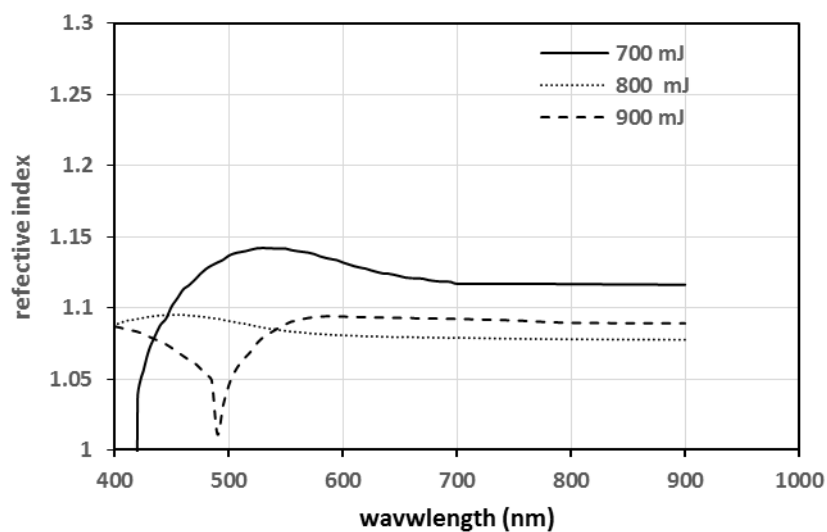


Fig.(10) :Variation of refractive index as a function of wavelength of Fe₂O₃ films for different deposition conditions

Both the real and imaginary parts of the dielectric constant versus the photon energy are illustrated in figure (11). The real part represents the amount of actual saving of electrical energy. While, the imaginary part represents the absorption losing associated with free carriers. The complex dielectric constant were calculated using Equations (10

and 11). The curves for both parts are found to be oscillatory in nature for all deposition conditions depending upon both of the crystal structure and the thickness of the prepared film. The curves in Figure (11) show similar behavior of those curves of extension coefficient due to the depending the values of (ϵ_i) on the concept of (K) [16].

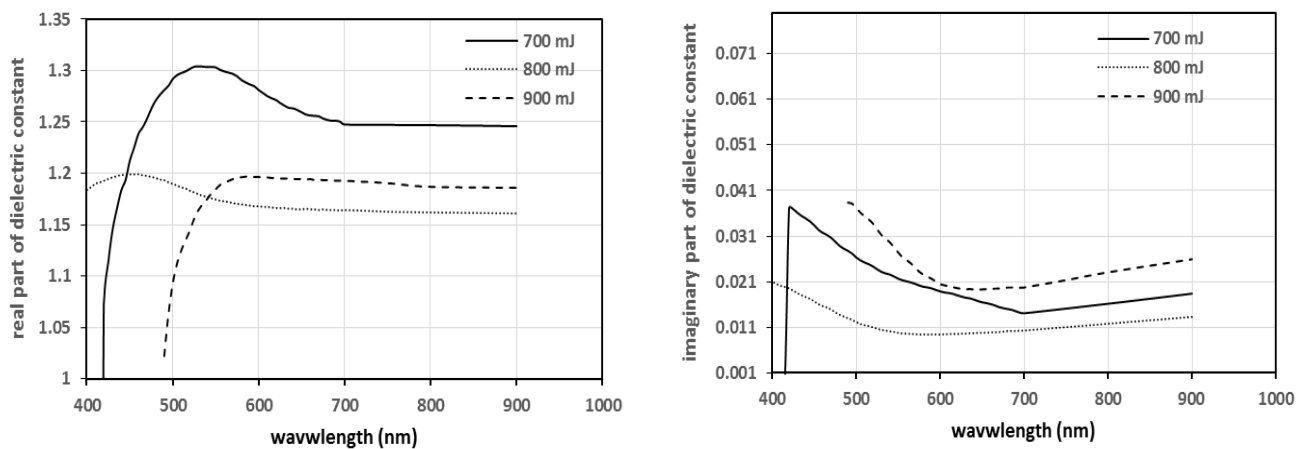


Fig.(11) : The real and imaginary part of dielectric constant versus wavelength of Fe_2O_3 films for different deposition conditions.

Conclusions:

In this paper we have reported the energy of laser pulses dependent optical properties of Fe_2O_3 thin films deposited by PLD method. The film thickness is changed from 63nm –

189nm, the GS was changed from 6.8nm –12.4 nm, with change in optical band gap from (2.28–2.8eV). The optimum energy to deposit nano Fe_2O_3 film for photovoltaic applications is about 800 mJ.

References:

- 1- I. Kazeminezhad and A. Sadollahkhani, *Mater. Lett.*, 2014,120, 267.
- 2- K. Vignesh, A. Suganthi, M. Rajarajan and S. A. Sara, *Powder Technol.*, 2012, 224, 331.
- 3- W. Lu, C. Jiang, D. Caudle, C. Tang, Q. Sun, J. Xu and J. Song, *Phys. Chem. Chem. Phys.*, 2013, 15, 13532.
- 4- A. Roychowdhury, S. Prakash Pati, S. Kumar and D. Das, *Powder Technol.*, 2014, 254, 583.
- 5- Z. Zeng, C. S. Garoufalis, A. F. Terzis and S. Baskoutas, *J.Appl. Phys.*, 2013, 114, 23510.
- 6- P. Liu, Y. Li, Y. Guo and Z. Zhang, *Nanoscale Res. Lett.*, 2012, 7, 220.
- 7- X. Xu, M. Wu, M. Asoro, P. J. Ferreira and D. L. Fan, *Cryst. Growth Des.*, 2012, 12, 4829.
- 8- S. Sahare, S. J. Dhoble, P. Singh and M. Ramrakhiani, *Adv.Mater. Lett.*, 2013, 4, 169.
- 9- W. H. Nam, Y. S. Lim, W. S. Seo and J. Y. Lee, *Philos. Mag.*,2013, 3, 4221.
- 10- X. Zhang, M. L. Chen, J. Wen, L. L. Wu, H. Gao and D. Zhang, *CrystEngComm*, 2013, 15, 1908.
- 11- B. H. Ahn and J. Y. Lee, *CrystEngComm*, 2013, 15, 6709 .
- 12- Y. Liao, C. Xie, Y. Liu, H. Chen, H. Li and J. Wu, *Ceram. Int.*, 2012, 38, 4437–4444 .
- 13- Y. H. Mun, S. H. Park, H. S. Ko and C. M. Lee, *J. Korean Phys.Soc.*, 2013, 63, 1595.
- 14- S. Suwanboon, P. Amornpitoksuk, A. Sukolrat and N. Muensit, *Ceram. Int.*, 2013, 39, 2811–2819.
- 15- S. M. Lam, J. C. Sin, A. Z. Abdullah and A. R. Mohamed, *Desalin. Water Treat.*, 2012, 41, 131–169 .
- 16- S. Ameen, H. K. Seo, S. M. Akhtar and H. S. Shin, *Chem. Eng.J.*, 2012, 210, 220–228.